Earthquakes and Structures, *Vol. 10, No. 4 (2016) 757-768*
DOI: http://dx.doi.org/10.12989/eas.2016.10.4.757

Effect of near field earthquake on the monuments adjacent to underground tunnels using hybrid FEA-ANN technique

Mohsen Jafarnia[*1] and Mehdi Imani Varzaghani[2a]

[1]*Faculty of Engineering, Central Tehran Branch - Islamic Azad University, No. 49 Mofatteh Ave. Tehran, Iran*
[2]*Faculty of Engineering, Kharazmi University, No. 1 orag Ave., Tehran, Iran*

(Received December 24, 2014, Revised December 7, 2015, Accepted December 16, 2015)

Abstract. In the past decades, effect of near field earthquake on the historical monuments has attracted the attention of researchers. So, many analyses in this regard have been presented. Tunnels as vital arteries play an important role in management after the earthquake crisis. However, digging tunnels and seismic effects of earthquake on the historical monuments have always been a challenge between engineers and historical supporters. So, in a case study, effect of near field earthquake on the historical monument was investigated. For this research, Finite Element Analysis (FEM) in soil environment and soil-structure interaction was used. In Plaxis 2D software, different accelerograms of near field earthquake were applied to the geometric definition. Analysis validations were performed based on the previous numerical studies. Creating a non-linear relationship with space parameter, time, angular and numerical model outputs was of practical and critical importance. Hence, artificial Neural Network (ANN) was used and two linear layers and Tansig function were considered. Accuracy of the results was approved by the appropriate statistical test. Results of the study showed that buildings near and far from the tunnel had a special seismic behavior. Scattering of seismic waves on the underground tunnels on the adjacent buildings was influenced by their distance from the tunnel. Finally, a static test expressed optimal convergence of neural network and Plaxis.

Keywords: soil-structure interaction; tunnel; historical monuments; artificial neural network (ANN); near field earthquake

1. Introduction

Near field earthquake was introduced since the Parkfield 1966 earthquake in California for the first time. In recent decades, many studies on the structural behavior near faults have been presented. Azarhoosh and Amiri (2010) have assumed that the structure is located on a rigid soil, with increasing the soil flexibility, there will be significant variations in the structural response, i.e., the effects of Soil-Structure Interaction (SSI). It is concluded that under SSI effects there are clear similarities between elastic demands subjected to pulse-type, and near-fault motions. An analytical study by Tornello and Sarrazin (2012) have investigated a base isolation for three-story building subjected to near-fault earthquakes and compared with experimental results. The results

*Corresponding author, E-mail: mohsenj146@gmail.com
[a]Student researcher, E-mail: mehdiimani1987@yahoo.com

http://www.techno-press.com/journals/eas&subpage=7 ISSN: 2092-7614 (Print), 2092-7622 (Online)

show that the spring-based system can be an alternative for base isolation of small building located near active faults. Eleftheriadou and Karabinis (2012) have been a comprehensive study on the seismic vulnerability assessment of typical building types, representative of the structural materials, the seismic codes and the construction techniques of Southern Europe. They have drawn on the parameters that influence the seismic response based on the wide homogeneous database which have shown reduction of scatter on the produced results. Liu *et al*. (2012) proposed separate models for evaluating the behavior of unreinforced materials; it was a practical tool and was relatively simple in designing evaluation of vulnerability-reinforced structures. Ural (2013) have been a site survey of masonry damages that is presented Response Spectrum Analysis of the Halil Aga Mosque by using the finite element method.

Effection of tunneling on historical and masonry buildings have been studied in static situation by researchers such as Rampello *et al*. (2012), Farrell *et al*. (2013) and Giardina *et al*. (2014). On the other hand, according to the reports presented about the destructive effects of earthquakes on underground structures such as the Kobe earthquake in 1995, 1999 Taiwan Chi Chi, and Turkey Cocali, soil as an effective factor between the surface and underground can have transmission destructive effects on the surface structures adjacent to tunnels. Liu *et al*. (2010) have presented test results of a prototype model of soil and metro tunnel interaction on a 1/40 scale in laboratory. One of the results is described that the tunnel-soil interaction had significant influence on the bulk dynamic response of the system. Manolis *et al*. (2013) have studied seismically induced, anti-plane strain wave motion in a non-homogeneous geological region containing tunnels by a hybrid computational technique. On the base of results, the hybrid FDM-BEM technique is able to quantify dependence of the signals that develop at the free surface to the following key parameters: seismic source properties and heterogeneous structure of the wave path. Baziar *et al*. (2014) by using dynamic centrifuge tests and numerical simulations of the same tests have studied the seismic behavior of buried box tunnels. The results of seismic studies are shown interaction between underground tunnel-ground surface. Therefore, seismic behavior of monuments was investigated adjacent to the tunnels during near field earthquakes in this paper.

2. Research methodology

In this study, finite element analysis was used for the analysis of soil-structure interaction during near field earthquakes. For this analysis, Plaxis 2D software in dynamic mode was used. Plane strain model was selected in Plaxis. Earthquake loads were applied at the bottom of the model as acceleration. For engineering understanding from the seismic behavior of the monuments, neural network analysis was used. Neural networks are composed of simple elements operating in parallel. These elements are inspired by biological nervous systems. As in nature, the network function is determined largely by the connections between elements. We can train a neural network to perform a particular function by adjusting the values of the connections between elements. Commonly neural networks are adjusted, or trained, so that a particular input leads to a specific target output. The network is adjusted, based on a comparison of the output and the target, until the network output matches the target. Tansig is One of the used functions in neural network. Tansig is a transfer function. Transfer functions calculate a layer’s output from its net input. Therefore, using two linear layers, Tansig function, and changes in the number of neurons were performed in the neural network analysis.

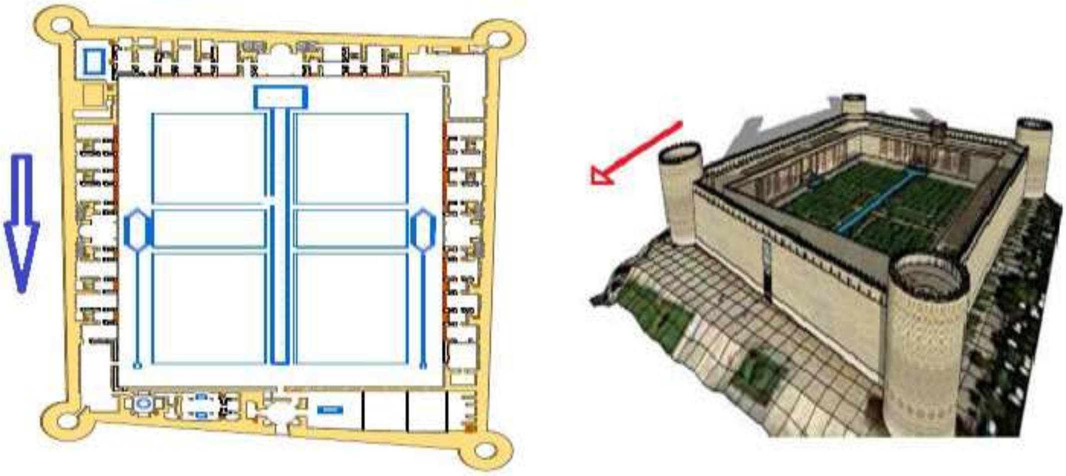

Fig. 1 Plan of the ground floor and three-dimensional view of Arg-e-Karim Khan

3. Case study

This research was conducted in city of Shiraz, Iran. As shown in Fig. 1, the studied area was the tunnel of Line 1 subway in Shiraz. Subway tunnels pass under Zand underpass near Arg-e-Karim Khan. The arrow shows the direction of the subway tunnels to the nearest wall of Arg.

4. Geology and geotechnology of the zone

In the geological study, it was found that route of Line 1 consisted of two thick alluvium composed of particles of different sizes. In Table 1, soil properties of site and laboratory tests are presented. Soil classification was based on the Unified Soil Classification. In the numerical analysis, Mohr-Coulomb model was considered for soil. Considering that, in earthquake, materials have no drain opportunities, undrainage materials were defined. Groundwater level was approximately 6.5 m above the crown of the tunnel (Fig. 2). The type of contact between layers of soil is considered permanent in Plaxis 2D. Also, Load traffic is determined on the basis of valid data in the journal paper that have been studied by Afifipour *et al*. (2011) in the same area of Shiraz.

5. Analysis in the Plaxis 2D

Geometry and the 15-node triangular mesh are shown in Fig. 3. The dimensions of model is 370 m and 40 m in length and depths, repectively. Due to the importance of structural-soil behavior around the tunnels and structures, mesh size must be finer. For this purpose, inside clusters in the tunnels and buildings were selected. Then the Refine cluster option was used to generate mesh in Plaxis 2D. Afterward the plates representing the structures and tunnels were selected and the Refine line option from the mesh menu was clicked to generate mesh. According to the studied area, Tabas and Northridge near field earthquakes were selected. Modeling of the area's structures was studied and the earthquake-angle was applied to model geometry, as shown in Fig. 4 as an example.

Table 1 Soil Properties

No. layers	Depth (m)	Type Of Soil	Saturated Unit Weight (kN/m^3)	Unit Weight (kN/m^3)	Cohesion (kN/m^2)	Angle of Internal Friction (degree)	Elastic modulus (kN/m^2)	Poisson's Ratio	Riley coefficient, α, β
1	0-4	SC	18.64	15.7	30	33	32500	0.3	0. 022, 0.0099
2	4-7.2	CL-ML	20.4	16.8	40	29	50000	0.25	0. 022, 0.0099
3	7.2-13.9	ML	20.5	16.48	10	32	30000	0.25	0. 029, 0.003
4	13.9-16.9	CL	20.4	16.8	20	29	50000	0.25	0. 027, 0.006
5	16.9-18.7	CL-ML	20.5	16.58	10	32	50000	0.25	0. 024, 0.0079
6	18.7-**40**	SM-ML	20.5	17.36	10	29	50000	0.25	0. 024, 0.0049

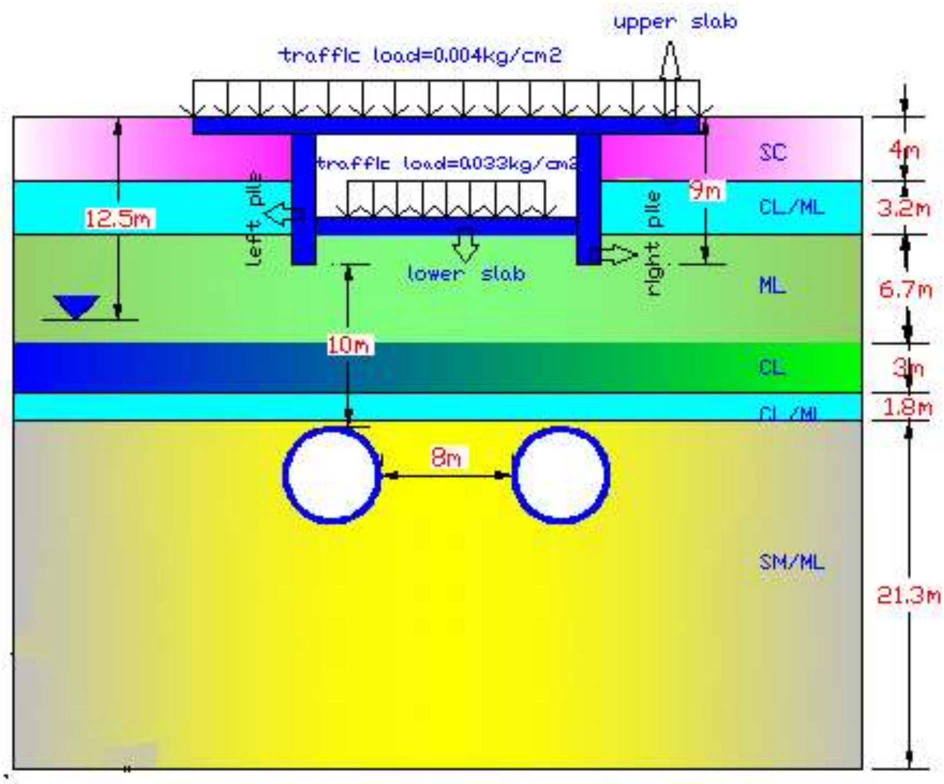

Fig. 2 Thickness of the soil layer and distribution of traffic load on the transition

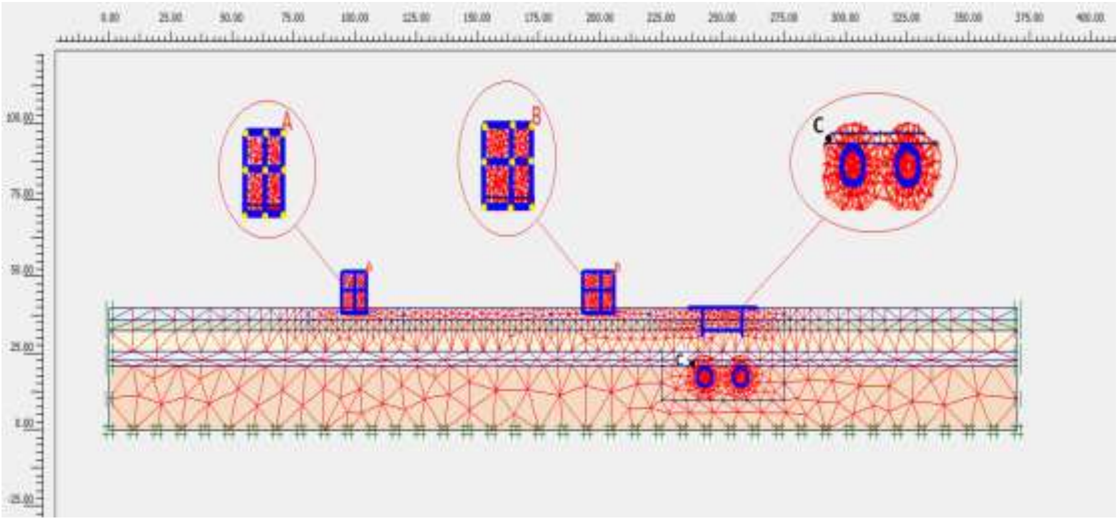

Fig. 3 Dimensions and final mesh of geometric model in Plaxis

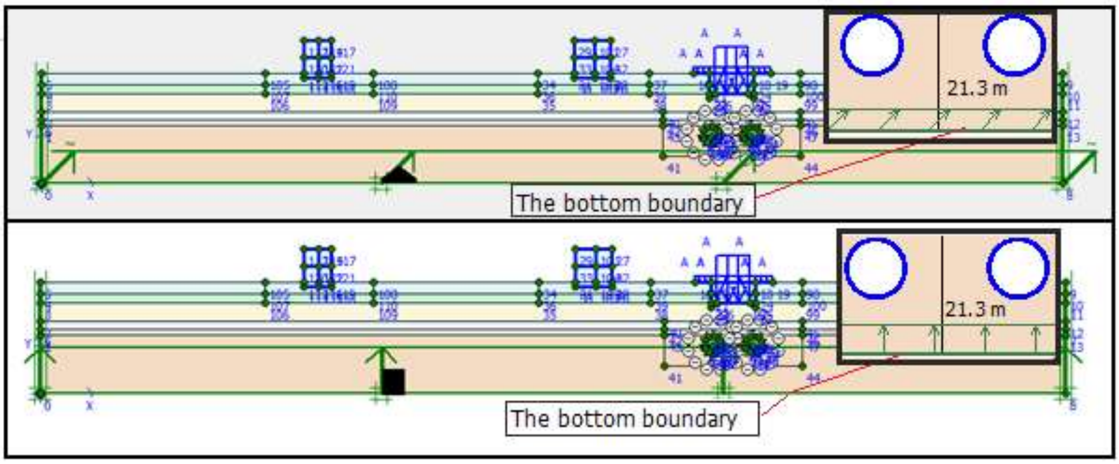

Fig. 4 modeled earthquake with 45 and 90 degrees at the bottom boundary

Accelerograms of Tabas and Northridge areas were selected from PEER NGA (Pacific Earthquake Engineering Research Center) considering the zone soil. From this record, 20 s of accelerograms that had more critical state were used for dynamic analysis in the Plaxis 2D. Since Shiraz city is among the areas with high seismicity, acceleration records were modified to 0.3 g according to 2800 code of Iran. Modified accelerograms are presented in Fig. 5.

The inner and outer diameters of the tunnels were 6.3 m and 6.6 m, respectively. Width of the top and bottom concrete slab underpasses were 28 m and 16 m, respectively, and length of concrete piles underpass was 8.2 m. Distance between the tunnels and traffic load distribution is shown in Fig. 2. The tunnel lining was made of pre-stressed concrete segments. Closer and farther building distances from the closest axis of the tunnel were 37 m and 138 m, respectively. In Tables 2-4, necessary properties of constructs were given for modeling in Plaxis. Sensitivity analysis was performed on the mesh boundary.

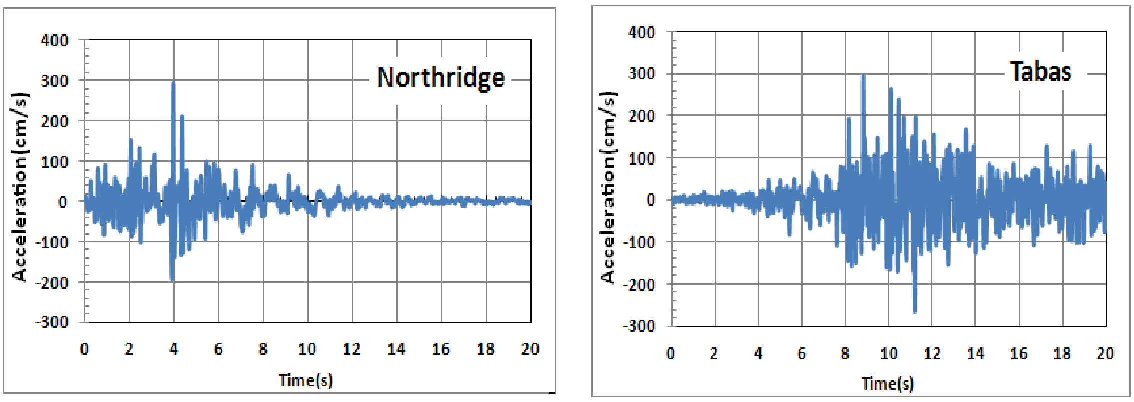

Fig. 5 Accelerograms of two modified near field earthquakes

Table 2 Properties of underpass materials and tunnel lining

Type of structure	Type of material	Bending stiffness (kN.m^2/m)	Axial stiffness (kN/m)	Weight (kN/m/m)	Thickness (m)	Poisson's Ratio	Behavioral Model
Lining	concrete	706000	942000	7.5	0.3	0.1	Elastic
Slab underpass	concrete	1109000	208000000	19	0.8	0.15	Elastic
Pile of underpasses	concrete	3744000	31200000	28	1.2	0.15	Elastic

Table 3 Properties of materials for closer building to the tunnel

Type of structure	Type of material	Bending stiffness (kN.m2/m)	Axial stiffness (kN/m)	Weight (kN/m/m)	Thickness (m)	Poisson's Ratio	Behavioral Model
Right wall	masonry	10920000	12800000	48	3/2	0.3	Elastic
Left wall	masonry	11980000	13200000	49/5	3/3	0.3	Elastic
Middle wall	masonry	34610000	18800000	70/5	4/7	0.3	Elastic
Building roof	masonry	1120000	6000000	22	1/5	0.3	Elastic
Building floor	masonry	41670	2000000	7/5	0/5	0.3	Elastic

Table 4 Properties of materials for farther building from the tunnel

Type of structure	Type of material	Bending stiffness (kN.m^2/m)	Axial stiffness (kN/m)	Weight (kN/m/m)	Thickness (m)	Poisson's Ratio	Behavioral Model
Right wall	masonry	7317000	11200000	42	2/8	0.3	Elastic
Left wall	masonry	11980000	13200000	49/5	3/3	0.3	Elastic
Middle wall	masonry	28390000	17600000	66	4/4	0.3	Elastic
Building roof	masonry	1120000	6000000	22	1/5	0.3	Elastic
Building floor	masonry	41670	2000000	7/5	0/5	0.3	Elastic

of near field earthquakes are presented in the following cases.

6. Investigating seismic behavior of Arg buildings in the vicinity of subway tunnel

To investigate the seismic behavior of Arg buildings, Tabas and Northridge earthquake were applied to geometry models with 45 and 90 angles. Model building far from the tunnel was done in two modes as follow:

1) The building far from the tunnel was modeled based on reality data (Table 4).

2) The building far from the tunnel was modeled similar to the nearby building (Table 3).

Selected points in the analysis of Plaxis 2D were (A, B) (Fig. 3).

7. Effect of the tunnel on further building

Considering that increase in weight during an earthquake can increase the destructive interaction of structures and soil, , building far from the tunnel were modeled similar to closer building in case 2. In other words, further building to tunnels has been heavier than case 1. To investigate interaction between tunnel-further building, sig'-1 effective stress of point c (Fig. 3) in vicinity tunnel and earthquakes with a 90 degree angle has considered.

8. Finding a suitable neural network

Each of the earthquakes with 45 and 90 angles were applied to the geometry of the model. In addition, earthquakes with 54 angle was applied to increase input data in the neural network. Therefore, probability of achieving the appropriate neural network increases. 18 points were selected for analysis at the intersection of buildings (see yellow points on the buildings in Fig. 3. 18 points were selected for analysis at the intersection of buildings (see yellow points on the buildings in Fig. 3). Input and output parameters were selected on the basis of two factors. First is knowing some input parameters without referring to the output of numerical analysis. Second is iterating the different compounds of parameters to find a suitable network. The output parameters of the neural network included (u_x/u_t) and input parameters were (u_y/u_t), $(x/(x+y))\times(t/20)$, $(t/20)\times(\alpha/360)$. *X*, *y*, *t*, u_x, u_y, and u_t are coordinates of the horizontal and vertical, time spent after earthquake, displacement in the horizontal and vertical direction, and absolute value of displacement, respectively. Input and output parameter values were normalized. 10% of the input data was kept for testing. Tansig function in neural networks and linear double-layer analysis were considered. Then, by changing the number of neurons, different networks were obtained for each set of analysis. Each of the networks with minimum MSE for test data was the desirable network. Accuracy of the results of the selected network with Plaxis results were analysed by Mann-Whitney test.

9. Results

9.1 Behavior of near and far buildings to tunnels during near field earthquakes

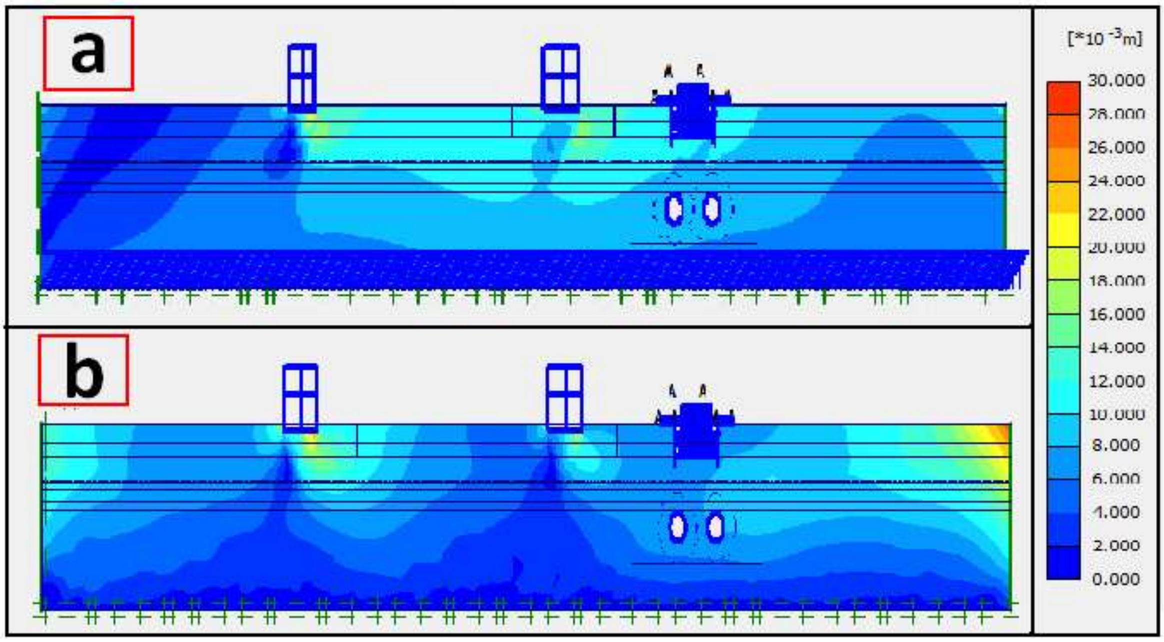

Fig. 6 Distribution of total displacement in soil

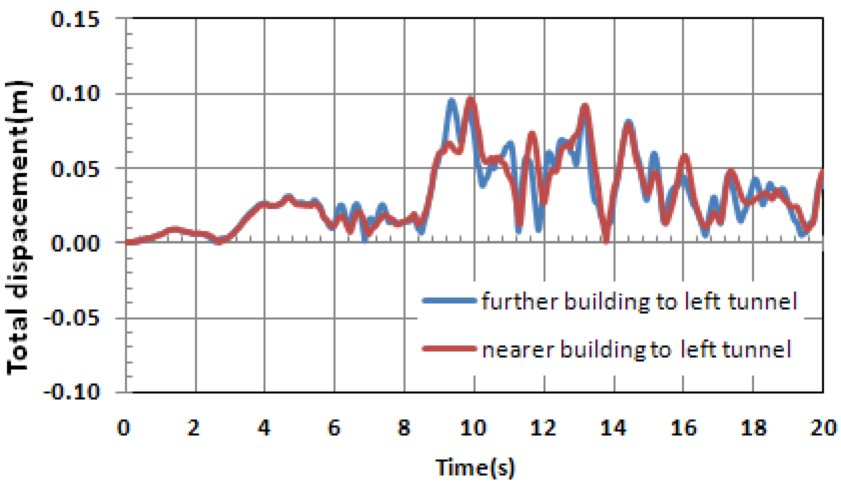

Fig. 7 Total displacement-time charts in Tabas earthquake for points A and B (see Fig. 3)

Examples of the displacement distribution in the soil due to earthquake loading in cases 1 and 2 are given in Fig. 6. In Fig. 7, one of the total displacement charts is presented for point A and B in buildings (see Fig. 3). In the earthquake different cases to compare the behavior of near and far buildings, Mann-Whitney test was used in case 1.

Diagram (a) is related to Northridge earthquake with a 45 degree angle in the geometry model in case 1. Diagram (b) is related to Tabas earthquake an applied 45 degree angle in the geometry model in case 2.

Results of Mann-Whitney test in comparison with near and far building in different cases of earthquakes were almost zero. According to p-value<0.05, it is clear that far and near buildings showed particular seismic behavior during earthquakes. In other words, the location of the buildings in the seismic behavior of the model was influenced. For each period of the earthquake, there was a certain corresponding value of displacement. Then, for understanding the changes of both point A and B (Fig. 3) in buildings, the bar graph was applied (Fig. 8). The percentage used in bar graph was obtained the following description.

If suppose F In any case of earthquake is number of the times at which the point B of the closer building was higher in terms of corresponding total displacement than the farther building (point A) and M is Number of time intervals (given the time intervals of 0.02 sec for the cost of an earthquake, M equals 1000) Then each of the bar graph was obtained while F divided to M. Also, to compare the behavior of near and far buildings during earthquakes, maximum corresponding value of displacement in the points A and B in buildings is given in Tables 5-6.

From the bar graph in Fig. 9 and Table 5, the following results can be deduced:

1) As shown in in Table 5, maximum corresponding total displacement in case 1 in the farther building, except one case, had a critical value compared with the closer building. But in case 2,

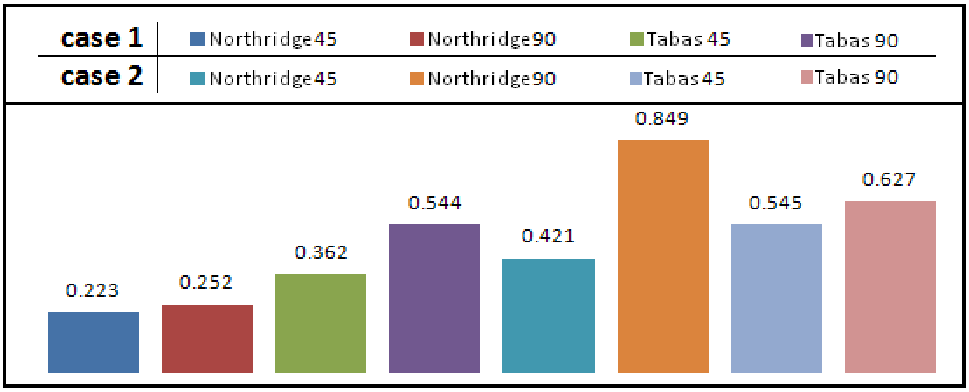

Fig. 8 The percent of times at which the top right point of the closer building was higher in terms of corresponding total displacement than the farther building

Table 5 Maximum corresponding total displacement for points A and B in the buildings

Earthquake Name	Angle Of Earthquake	Point Name	Total Displacement case 1 (cm)	Total Displacement case 2 (cm)
Tabas	45	A	12/9	10/5
Tabas	45	B	12/2	12/2
Tabas	90	A	9	8/9
Tabas	90	B	9/6	9/5
Northridge	45	A	10/5	8/9
Northridge	45	B	9/2	9/2
Northridge	90	A	6/9	5/2
Northridge	90	B	6/4	6/5

the closer building had more critical values. Also, according to the bar graph in case 2, the closer building had a more critical mode in terms of the number of time intervals than case 1. One of the above results refers to dimensions and weight of the far building was the same as that of the closer building to the tunnels. In other words, the farther building was heavier than case 1.

2) In each of the cases 1 and 2 for each of the earthquakes at the same angles, maximum corresponding value of displacement differed, which represent that types of earthquakes (amount of accelerograms) affect the behavior of structures.

3) From case 1's bar graph, it can be found that, if the angle of the applied earthquake to geometry model increased, the closer building would show critical behaviors in a more number of time intervals than the farther building. According to the results in Table 5, values of maximum displacement decreased with angle increase. Therefore, angle of earthquake actions in the geometry model was a factor affecting the behavior of the near and far buildings.

9.2 Effect of tunnel on the farther building

In Fig. 9, instances of the stress distribution in the soil due to earthquakes are presented. Diagram (a) is related to Northridge earthquake in case 2 that actions with a 90 degree angle in the geometry model. Diagram (b) is related to Tabas earthquake in case 1 that actions with a 90 degree angle in the geometry model. To compare results of analysis for point c (Fig. 3), Mann-Whitney test has been used. Resulted has been shown in Table 6.

Due to the convergence achieved in results, effect of scattering of seismic waves on the far building seemed to be very small. In other words, soil-tunnel interaction induced a very little effect on the farther building.

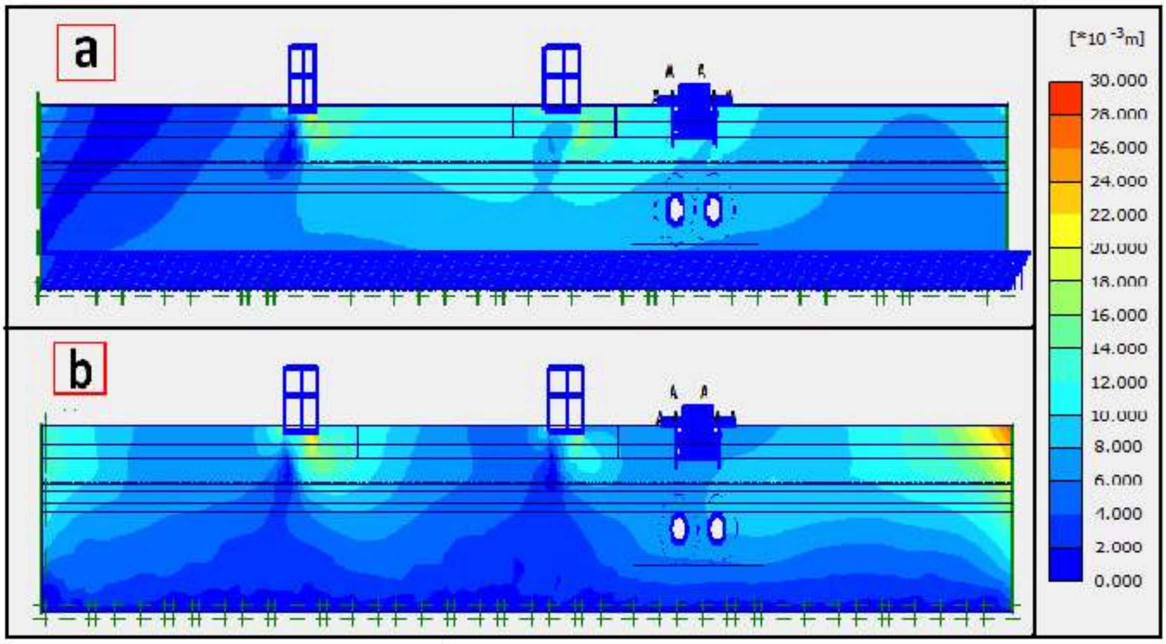

Fig. 9 Total stress distribution in soil

Table 6 Results of Mann-Whitney test in comparison sig'-1 effective stress in around tunnel (point c, see Fig. 3)

The name of earthquake	Tabas	Northridge
Comparison between case1 with case 2	P-value=0.93>0.05	P-value=0.99>0.05

9.3 Best neural network

According to the analysis on the neural network, the network with five neurons was the best one. Then, using Mann-Whitney test, results of neural networks were evaluated using Plaxis results. Amount of p value was 0.917, which showed the accuracy of the neural network results.

10. Conclusions

Earthquakes in the monuments near the underground tunnels were studied. Behavior of Karim Khan Buildings which were in the vicinity of subway tunnels during the earthquake in Plaxis 2d was also analyzed. Accelerograms of the earthquake engineering environment were applied and the displacement obtained from different parts of the buildings during earthquakes was used for neuralnetwork analysis. Also, for having an engineering vision from the seismic behavior of Arg Building (buildings around the area near the tunnel), the network with 5 neurons was selected and Mann-Whitney test confirmed the accuracy of the results. Comparison of the maximum total displacement in points A and B in the buildings (see Fig. 3) showed that there are some factors required to judge proper regarding the seismic behavior of monuments. These factors that should be considered simultaneously are applied earthquake angles in the model geometry, accelerograms of earthquake, size and weight of the buildings, and distance of buildings from underground tunnels. According to the case study, the farther Arg Building (at the distanceof 138 m from the axis of the closer tunnel) was protected from the damaging effect of tunnels during earthquakes.

References

Azarhoosh, Z. and Amiri, R.G. (2010), “Elastic response of soil-structure systems subjected to near-fault rupture directivity pulses”, *Proceedings of GeoShanghai International Conference*, Shanghai, China.

Tornello, M.E. and Sarrazin, M. (2012), “Base-isolated building with high-damping spring system subjected to near fault earthquakes”, *Earthq. Struct.*, **3**(3), 315-340.

Eleftheriadou, A.K. and Karabinis, A.I. (2012), “Seismic vulnerability assessment of buildings based on damage data after a near field earthquake (7 September 1999 Athens-Greece)”, *Earthq. Struct.*, **3**(2), 117-140.

Liu, T., Luan, Y. and Zhong, W. (2012), “Earthquake responses of clusters of building structures caused by a near-field thrust fault”, *Soil Dyn. Earthq. Eng.*, **42**(1), 56-70.

Ural, A. (2013), “19th May 2011 Simav (Kütahya) earthquake and response of masonry Halil Aga Mosque”, *Earthq. Struct.*, **4**(6), 671-683.

Rampello, S., Callisto, L., Viggiani, G. and Soccodato, F.M. (2012), “Evaluating the effects of tunnelling on historical buildings: the example of a new subway in Rome/Auswertung der Auswirkungen des Tunnelbaus auf historische Gebäude am Beispiel einer neuen U-Bahnlinie in Rom”, *Geomech. Tunnel.*, **5**(3), 275-299.

Giardina, G., Hendriks, M. and Rots, J. (2014), “Damage functions for the vulnerability assessment of

masonry buildings subjected to tunneling", *Struct. Eng.*, **140**(10), 04014212.
Farrell, R., Mair, R., Sciotti, A. and Pigorini, A. (2013), "Building response to tunnelling", *Soil. Found.*, **54**(3), 269-279.
Liu, N., Liu, Y., Han, D., Men, Y. and Peng, J. (2010), "Prototype model tests of soil and tunnel interactions under earthquake forces", *Proceeding of Tenth International Conference of ChineseTransportation Professionals (ICCTP)*, Beijing, China.
Manolis, G.D., Makra, K., Dineva, P.S. and Rangelov, T.V. (2013), "Seismic motions in a non-homogeneous soil deposit with tunnels by a hybrid computational technique", *Earthq. Struct.,* **5**(2), 161-205.
Baziar, M.H., Moghadam, M.R., Kim, D.S. and Choo, Y.W. (2014), "Effect of underground tunnel on the ground surface acceleration", *Tunnel. Undergr. Space Technol.*, **44**(1), 10-12.
Afifipour, A., Sharifzadeh, M., Shahriar, K. and Jamshidi, H. (2011), "Interaction of twin tunnels and shallow foundation at Zand underpass, Shiraz metro, Iran", *Tunnel. Undergr. Space Technol*., **26**(2), 356-363.

CC